
Task-Balanced Batch Normalization for Exemplar-based Class-Incremental Learning

Sungmin Cha^{1,2} Soonwon Hong¹ Moontae Lee^{2,3} Taesup Moon¹

Abstract

Batch Normalization (BN) is an essential layer for training neural network models in various computer vision tasks. It has been widely used in continual learning scenarios with little discussion, but we find that BN should be carefully applied, particularly for the exemplar memory based class incremental learning (CIL). We first analyze that the empirical mean and variance obtained for normalization in a BN layer become highly biased toward the current task. To tackle its significant problems in training and test phases, we propose Task-Balanced Batch Normalization (TBBN). Given each mini-batch imbalanced between the current and previous tasks, TBBN first reshapes and repeats the batch, calculating near task-balanced mean and variance. Second, we show that when the affine transformation parameters of BN are learned from a reshaped feature map, they become less-biased toward the current task. Based on our extensive CIL experiments with CIFAR-100 and ImageNet-100 datasets, we demonstrate that our TBBN is easily applicable to most of existing exemplar-based CIL algorithms, improving their performance by decreasing the forgetting on the previous tasks.

1. Introduction

Continual learning (CL) from sequentially accessible datasets for neural networks has been actively studied in recent years, because of its efficiency: eliminating the process of re-training from scratch whenever a new dataset is added (Delange et al., 2021). However, since the model is only trained by a dataset from the current task or an im-

balanced dataset between the current and previous tasks, a neural network-based model that performs CL suffers from the serious trade-off between stability and plasticity (Mermillod et al., 2013). To overcome this trade-off, various studies have been focused to alleviate forgetting in weights of the neural network model during CL (Delange et al., 2021; Parisi et al., 2019; Chaudhry et al., 2018).

CL is categorized into three types, such as task-, domain- and class-incremental learning (CIL) (Van de Ven & Tolias, 2019), and CIL has recently attracted more attention due to its efficiency that a task-ID is not required at inference time. In both online and offline CIL, many studies have suggested various methods to overcome the common cause of forgetting in CIL called biased prediction (Masana et al., 2020; Mai, 2021). Despite the many achievements of online CIL methods, these methods still have the disadvantage of reaching superior results only in a simple datasets, such as CIFAR-100 (Krizhevsky et al., 2009). Many studies have been conducted with the goal of successful offline CIL, however, it is turned out that offline CIL more suffers from serious forgetting and biased prediction than online CIL due to training with many epochs (Belouadah & Popescu, 2019). As a result, bias correction-based methods with exemplar memory has become the mainstream of offline CIL (Wu et al., 2019; Belouadah & Popescu, 2019; Ahn et al., 2021). These achieve superior results in not only a simple dataset but also a large-scale dataset such as ImageNet-100 or ImageNet-Full (Deng et al., 2009).

On the other hand, little discussion has been made on the neural network model applying to CIL. In particular, the most recent models (*e.g.*, ResNet-18 (He et al., 2016)) contain Batch Normalization (BN) layer, which is originally designed for the case of training a single task, so it is necessary to reconsider the proper use of BN in CIL. Recently, Continual Normalization (CN) (Anonymous, 2022) points out the problem of BN in online CL and CIL but it is still an open question what adverse effects BN has on offline CIL.

In this paper, we discuss the problem of BN in exemplar-based CIL which is the mainstream method of offline CIL. We show that the original BN causes a significant problem in calculating a mean and variance when it applied in exemplar-based CIL. The mean and variance are highly biased toward

¹Department of Electrical and Computer Engineering, Seoul National University, Seoul, Republic of Korea ²Fundamental Research Lab, LG AI Research, Seoul, Republic of Korea ³Information and Decision Sciences, University of Illinois at Chicago, Chicago, Illinois, USA. Correspondence to: Taesup Moon <tsmoon@snu.ac.kr>.

the current task, as a result, it makes the problem at normalization in both the training and test phase. To solve this problem, we propose Task-Balanced Batch Normalization (TBBN) consisting of two novel components, such as task-balanced mean and variance calculation and less-biased learning of parameters for affine transformation. For task-balanced mean and variance calculation, we propose a novel way to reorganize a given input of the BN layer so that mean and variance can be calculated in a task-balanced and adaptive way. Also, we devise less-biased learning of parameters for affine transformation, motivated by Ghost Batch Normalization (Hoffer et al., 2017), and we analytically show that it makes parameters to be trained in a less biased direction to current task in exemplar-based CIL. From extensive experiments with CIFAR-100 and ImageNet-100 datasets in short and long task sequence scenarios, first, we experimentally demonstrate that the problem of BN is the hidden cause of biased predictions. Second, we observe that our TBBN can be easily applied to various existing exemplar-based CIL methods and makes to improve their performance of them by reducing forgetting, without any requirement of searching a hyperparameter. Third, we show a simple fine-tuning with TBBN can surpass the performance of other sophisticated methods for CIL especially in the long task sequence scenario.

2. Related Work

Exemplar-based class-incremental learning For the first time, iCaRL (Rebuffi et al., 2017) proposed the exemplar-based CIL method, with nearest-mean-of-exemplars classification and representation learning. Also, they discussed some exemplar management ways such as random sampling and herding (Welling, 2009). EEIL (Castro et al., 2018) devised a distillation-based CIL method consisting of both balanced fine-tuning and representative memory updating, and they firstly reported an experimental result for the ImageNet (Deng et al., 2009) dataset. Different from previous methods, BiC (Wu et al., 2019) focused on biased prediction problem caused by a data imbalance issue of CIL, and they proposed a novel but simple idea which apply an additional layer for correcting biased prediction. LUCIR (Hou et al., 2019) started from the idea of LWF (Li & Hoiem, 2017), but they developed a more sophisticated loss function, based on cosine normalization, for overcoming catastrophic forgetting. Also, PODNet (Douillard et al., 2020) proposed another distillation-based method but they innovated in a way that focused more on a spatial-based loss for reducing a forgetting of representation. Recently proposed SS-IL (Ahn et al., 2021) analyzed that pure softmax mainly causes the biased prediction problem in CIL. Based on this findings, they proposed Separated Softmax and it has become the current state-of-the-art method.

Normalization layer An initial motivation of devising Batch Normalization (BN) (Ioffe & Szegedy, 2015) was trying to solve internal covariate shift. However, their belief in internal covariate shift was broken by follow-up studies, and the benefits from BN in terms of training perspective were analyzed in various directions (Bjorck et al., 2018; Santurkar et al., 2018). After that, several normalization layers devised for various computer vision tasks have been proposed with their respective advantage (Ulyanov et al., 2016; Wu & He, 2018; Hoffer et al., 2017). Recently, appropriate use of BN in more diverse tasks, such as meta-learning (Bronskill et al., 2020), task-incremental learning (Lee et al., 2020) and on-line class-incremental learning (Anonymous, 2022), have been discussed.

3. Notation and Preliminary

Notation We consider a general setting of class-incremental learning (CIL) by following the setting proposed in (Ahn et al., 2021). During CIL, a dataset \mathcal{D}_t for each task t incrementally arrives, and we set the total number of tasks to T . The dataset \mathcal{D}_t consists of pairs of an input image $\mathbf{x}_t \in \mathcal{X}$ and its target label y_t . We denote the total number of classes until t as $C_t = m \times t$ and assume that only m novel classes, which have been never seen before, are incrementally added at each task. Therefore, the target label of each task is labeled as $y_t \in \{C_{t-1} + 1, \dots, C_t\} \triangleq \mathcal{C}_t$. We use external memory for saving exemplars of previous tasks, and it is denoted by \mathcal{M} . The size of exemplar memory is set to not over $|\mathcal{M}|$ for whole incremental steps and exemplar memory is updated by a sampling algorithm after training each task. As a result, exemplar memory \mathcal{M}_{t-1} maintains $\lfloor \frac{|\mathcal{M}|}{C_{t-1}} \rfloor$ images per each past class and it is used for training task t . We consider a mini-batch size for training as $B = B_c + B_p$ where B_c and B_p denote the number of sampled data from \mathcal{D}_t and \mathcal{M}_{t-1} , respectively. We denote B numbers of sampled mini-batch data as $\mathbf{x}^B, y^B \sim \mathcal{D}_t, \mathcal{M}_{t-1}$ and consider that the sampled mini-batch data from \mathcal{D}_t and \mathcal{M}_{t-1} is sequentially concatenated, such as $\mathbf{x}^B = (\mathbf{x}^{B_c}, \mathbf{x}^{B_p}) = ((\mathbf{x}_1, \dots, \mathbf{x}_{B_c}), (\mathbf{x}_{B_c+1}, \dots, \mathbf{x}_{B_p}))$. Note that B_c is greater than B_p in typical CIL settings, and it is generally known that this imbalance causes a biased prediction problem for CIL (Ahn et al., 2021; Belouadah & Popescu, 2019; Wu et al., 2019). Therefore, we set the sampling ratio between B_c and B_p as $B_c : B_p = 3 : 1$ in our experiments. Additionally, we denote an input feature map for an intermediate BN layer when \mathbf{x}^B is given by $\mathbf{h} \in \mathbb{R}^{B \times C \times D}$, where C and D are the size of channels and a feature map respectively.

Batch normalization Batch Normalization (BN) (Ioffe & Szegedy, 2015) is one of the most famous normalization layers, which has been widely applied in various state-of-the-art neural network architectures (He et al., 2016; Szegedy et al.,

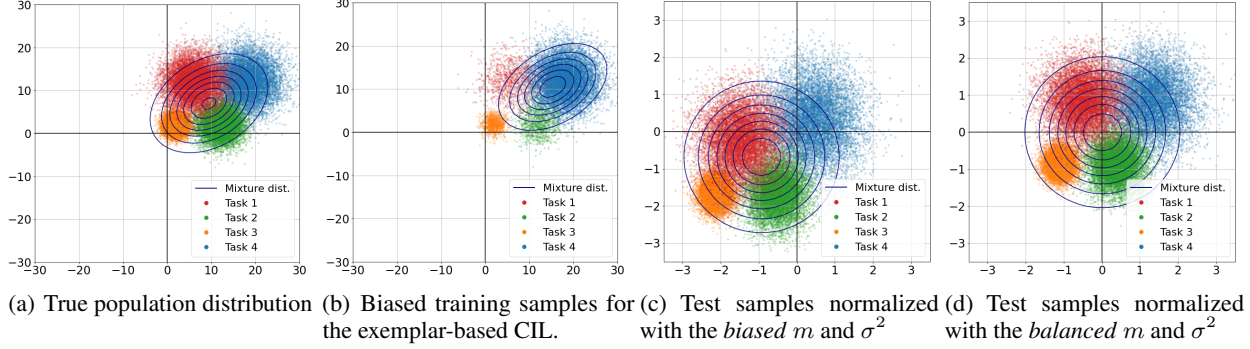


Figure 1: Illustration of the problem of BN in exemplar-based CIL.

2016; Tan & Le, 2019), due to its powerful practicality and efficiency. In the training phase, BN calculates an empirical mean and variance of the given mini-batch as:

$$\hat{\mu} = \frac{1}{BD} \sum_{b=1}^B \sum_{d=1}^D \mathbf{h}_{b,c,d}, \quad \hat{\sigma}^2 = \frac{1}{BD} \sum_{b=1}^B \sum_{d=1}^D (\mathbf{h}_{b,c,d} - \hat{\mu})^2 \quad (1)$$

where $\hat{\mu}, \hat{\sigma}^2 \in \mathbb{R}^C$. After that, \mathbf{h} is normalized by $\hat{\mu}$ and $\hat{\sigma}^2$, and then the normalized $\hat{\mathbf{h}} \sim \mathbb{N}(0, 1)$ is affine-transformed with a trainable parameter γ and β as below:

$$\hat{\mathbf{h}} = \frac{\mathbf{h} - \hat{\mu}}{\sqrt{\hat{\sigma}^2 + \epsilon}} \quad (2) \quad \mathbf{y} = \gamma \cdot \hat{\mathbf{h}} + \beta \quad (3)$$

where $\gamma, \beta \in \mathbb{R}^C$ and $\epsilon = 10^{-5}$. Note that, in a simple case where $D = 1$, γ and β are trained by a gradient:

$$\frac{\partial \mathcal{L}}{\partial \gamma} = \sum_{b=1}^B \frac{\partial \mathcal{L}}{\partial \mathbf{y}_b} \cdot \hat{\mathbf{h}}_b, \quad \frac{\partial \mathcal{L}}{\partial \beta} = \sum_{b=1}^B \frac{\partial \mathcal{L}}{\partial \mathbf{y}_b}, \quad (4)$$

where \mathcal{L} denotes a loss function.

For normalization in the test phase, running mean μ and variance σ^2 are incrementally updated at each training iteration i via exponential moving average, such as $\mu_i = m \cdot \hat{\mu} + (1-m) \cdot \mu_{i-1}$ and $\sigma_i^2 = m \cdot \hat{\sigma}^2 + (1-m) \cdot (V-1)/V \cdot \sigma_{i-1}^2$, where $V = B \cdot D$ is for vessel's correction.

4. Main Method

4.1. Motivation: Problem of BN in Exemplar-based CIL

The exemplar memory became an essential ingredient for achieving the state-of-the-art performance in offline CIL problems (Masana et al., 2020). However, in most recent work, the popular backbone classification models (e.g., ResNet-18 (He et al., 2016)) have been naively used without any discussion on the correct utilization of BN. One exception is the recent study in (Anonymous, 2022), but their so-called Continual Normalization was only evaluated in the online CL setting, and we show in the later section

that their method does not bring any significant gain in the more popular offline CIL setting.

To that end, in this section, we consider a motivating example and discuss that devising a correct BN mechanism for the exemplar memory-based CIL is necessary. Consider a synthetic input feature distribution for an intermediate BN layer shown in Figure 1. That is, Figure 1(a) visualizes 2-D data samples generated from the mixture of four different Gaussian distributions, each representing the feature distribution for each task. For a joint training setting, the mini-batch samples are uniformly sampled across four tasks, hence, the empirical mean and variance obtained for BN will get close to the true population mean and variance. Such mean and variance then will successfully standardize the samples in the mini-batch, both in training and test phases, through the ordinary BN process given in (2) and (3).

In contrast, for the exemplar memory-based CIL setting, there would be a severe imbalance in the samples in the training mini-batch since most samples would be coming from the current task (Task 4) as shown in Figure 1(b). Clearly, in this case, the mean and variance calculated by the BN layer would be biased toward those of the current task. In the test time of CIL, however, the test samples will be still balanced across the tasks as shown in Figure 1(c). Therefore, when the biased mean and variance obtained during training are used to normalize those test samples, the samples would not have the standardized distribution as shown in the figure. It is easy to imagine that such mismatch between the training and test sample distributions would cause the test performance deterioration since the trainable parameters of BN (i.e., γ and β) would be obtained for the normalized *training* samples. The obvious remedy for such mismatch would be to obtain the *task-balanced* empirical mean and variance during the training phase, and use them in the BN layer to normalize the test samples as shown in Figure 1(d).

In addition to the above mismatch between the training and test samples, a naive application of BN with the biased mini-batch samples would cause the problem solely for training

phase as well. That is, when the training for the current task (e.g., Task 4 in Figure 1) is finished, the empirical mean and variance obtained by a BN layer would be biased toward Task 4. However, when a new task (say, Task 5) arrives, since only a small sample of Task 4 data will be saved in the exemplar memory, the new empirical mean and variance, which will now get biased toward Task 5, would drift far away from the maintained ones so far (via the exponential moving average). This mismatch within the training phase would significantly alter the learned representation of the past task samples in the exemplar memory after the normalization, hence, it necessitates re-training of the weights of the subsequent layers, which unintentionally causes forgetting of the learned representations.

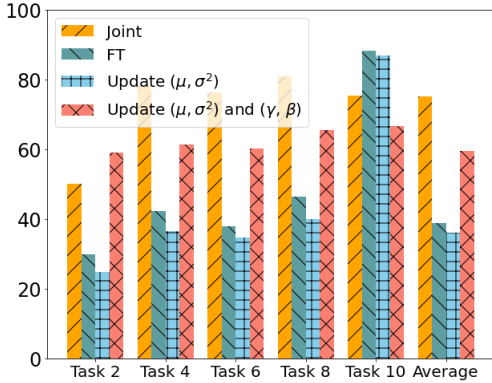


Figure 2: Experiments with ImageNet-100 ($|\mathcal{M}| = 2000$). With above two issues, we argue that it is critical to calculate the *task-balanced* mean and variance for BN layers in the exemplar memory based CIL problems. While a similar observation also has been made in the recent work (Anonymous, 2022), we go one step further and note that the affine transformation parameters of BN, γ and β in (3), should also be learned in a task-balanced way. To demonstrate such point, we experimented with ImageNet-100 dataset (broken down to 10 classes \times 10 tasks) using ResNet-18 architecture with the ordinary BN layer. Figure 2 reports the classification accuracy of every other task as well as the average accuracy across the tasks, computed after training the final task. “Joint” denotes the result of joint training of all task at once, which clearly gives the upper bound in most cases. On the other hand, “FT” is the fine-tuning baseline which simply fine-tunes the model with the current task and exemplar memory (of size 2000) data. Note it performs poorly on most past tasks except for the final task, clearly showing the biased prediction phenomenon. “Update (μ, σ^2)” is a synthetic scheme that *freezes* all trainable parameters of the obtained FT model and only re-calculates the running mean and variance of all BN layers using the whole dataset for all tasks (such that they are task-balanced). Finally, “Update (μ, σ^2) and (γ, β)” denotes another genie-aided scheme that also *re-trains* the (γ, β)’s for all BN layers with the whole task dataset together with updating (μ, σ^2)’s. From the fig-

ure, we observe that only obtaining the task-balanced (μ, σ^2) is not sufficient; in fact, “Update (μ, σ^2)” slightly hurts “FT” due to the mismatch between the updated (μ, σ^2) and the frozen (γ, β). In contrast, when the affine transformation parameters also become task-balanced, then we recognize that the overall average accuracy boost becomes significant. We stress that this is particularly interesting since the affine transformation parameters only take less than 1% of the entire model parameters, and simply making them and the empirical (μ, σ^2) used in BN layer task-balanced can bring a significant performance boost for a simple FT baseline. Motivated by this, we develop our Task-Balanced Batch Normalization (TBBN) layer in the next section.

4.2. Task-Balanced Batch Normalization

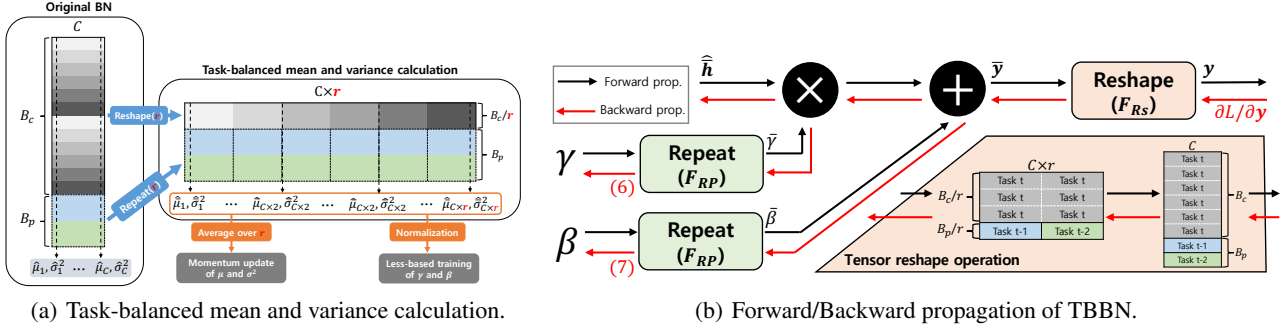
Our TBBN consists of two components: 1) Task-balanced μ and σ^2 calculation and 2) Less-biased training of γ and β .

Task-balanced mean and variance calculation The left mini-batch in Figure 3(a) illustrates how to calculate an empirical mean and variance (Equation (3)) in exemplar-based CIL. As discussed in the previous section, class imbalance between the current and previous data biases mean and variance toward the current task. Instead, we propose a task-balanced algorithm that better computes the empirical mean and variance in the current batch. As shown in Figure 3, we design the two different tensor operations: *reshape* and *repeat*, applying them to the current and previous parts, respectively. We determine the number of repeat/reshape operations r by the following Equation (5). Note that r is a hyperparameter, but the model provides a task-adaptive guidance without asking any exhaustive searching.

$$\frac{B_c}{r} : \frac{B_p}{t-1} = 1 : 1 \rightarrow r = \frac{B_c}{B_p} \cdot (t-1), \quad (5)$$

where $t = 2, \dots, T$, and r is set to 1 when $t = 1$.

Let \mathbf{x}^{B_c} be of the data sampled only from the current task t . After applying the reshape operation to \mathbf{x}^{B_c} with r , we divide \mathbf{x}^{B_c} into r splits, where each split has $\frac{B_c}{r}$ numbers of data from the current task. Let \mathbf{x}^{B_p} denote the data from the previous tasks. As \mathbf{x}^{B_p} consists of the data uniformly sampled from task 1 to $t-1$, $\frac{B_p}{t-1}$ numbers of data belongs to \mathbf{x}^{B_p} for each previous task in expectation. The key insight is that we can make every split balanced by repeating \mathbf{x}^{B_p} by r times if the task ratios $\frac{B_c}{r}$ and $\frac{B_p}{t-1}$ become equivalent. Then we calculate empirical mean $\hat{\mu} \in \mathbb{R}^{C \cdot r}$ and variance $\hat{\sigma}^2 \in \mathbb{R}^{C \cdot r}$ from a horizontally-concatenated task-balanced batch $\hat{\mathbf{x}} \in \mathbb{R}^{B_c/r + B_p \times C \cdot r \times D}$. Figure 3(a) shows the overall process of our proposed method. It is worth noting that this process is not affected by backpropagation. To update running mean $\mu \in \mathbb{R}^C$ and variance $\sigma^2 \in \mathbb{R}^C$ for test phase, we average $\hat{\mu}$ and $\hat{\sigma}^2$ over r splits, later applying these to exponential moving average for updating μ and σ^2 .



(a) Task-balanced mean and variance calculation.

(b) Forward/Backward propagation of TBBN.

Figure 3: Illustration for the components of TBBN. (b) shows the process of forward and backward propagation of TBBN for less-biased learning of γ and β , and the example of the tensor reshape operation. In this example, the gradient back-propagated from the next layer has a shape of $\partial \mathcal{L} / \partial \mathbf{y} \in \mathbb{R}^{B \times C}$, and it is reshaped into $F_{RS}^{-1}(\partial \mathcal{L} / \partial \mathbf{y}; r) \in \mathbb{R}^{B/r \times C \times r}$. As a result, the ratio between each previous task’s data and other task’s data (e.g., task $t-1$: other tasks = $1 : B-1$) is changed into task $t-1$: other tasks = $1 : B_c/r + B_p/r - 1$, becoming less-biased toward the current task.

Why does it work? Under the fixed memory size, individual mini-batches get dominated by the current task as t continually increases. As exponential moving average keeps averaging over empirical means and variances that are already biased toward the current task from the beginning, it cannot asymptotically recover population mean and variance even if learning averaging coefficients γ and β would alleviate the bias to some degrees. To acquire reasonable estimations for population statistics from the limited samples, it is necessary to reuse existing data samples with replacement from the previous task. In a nutshell, our TBBN reshapes \mathbf{x}^{B_c} and repeats \mathbf{x}^{B_p} , creating r task-balanced bags of bootstrapped samples, later approximating the population statistics by averaging bootstrap statistics.

Less-biased training of γ and β Additionally, we propose a way to train learnable parameters of BN (γ and β) in a more less-biased way to the current task. This method is motivated by Ghost Batch Normalization (GhostBN) (Hoffer et al., 2017), however, note that we first apply it in exemplar-based CIL and show its positive effect of it in an analytic manner.

After calculating the task-balanced $\hat{\mu}$ and $\hat{\sigma}^2$ from $\tilde{\mathbf{x}}$, we apply these to normalize a reshaped input feature map $\hat{\mathbf{h}} = F_{RS}(\mathbf{h}; r)$ via Equation (2), where F_{RS} is a tensor reshape function $F_{RS}(\mathbf{h}; r) : \mathbb{R}^{B \times C \times D} \rightarrow \mathbb{R}^{B/r \times C \times r \times D}$. Then, the normalized feature map $\hat{\mathbf{h}}$ is affine-transformed by Equation (3) with $\tilde{\gamma} = F_{RP}(\gamma)$ and $\tilde{\beta} = F_{RP}(\beta)$, where F_{RP} is a tensor repeat function $F_{RP}(\cdot; r) = [(\cdot)_1; \dots; (\cdot)_r] : \mathbb{R}^C \rightarrow \mathbb{R}^{C \cdot r}$. Finally, the affine-transformed feature map is re-shaped by the inverse of the tensor reshape function for recovering the original shape: $\mathbf{y} = F_{RS}^{-1}(\tilde{\mathbf{y}}) \in \mathbb{R}^{B \times C \times D}$ where $\tilde{\mathbf{y}} = \tilde{\gamma} \hat{\mathbf{h}} + \tilde{\beta}$, for transferring to a next layer.

We found that the above process makes a difference in the gradient for β and γ during backpropagation, compared to the original BN shown in Equation (3). Note that the gradient of the tensor reshape operation

F_{RS} is a reverse-direction-reshape of a given gradient \mathbf{g} : $F_{RS,g}(\mathbf{g}; r) : \mathbb{R}^{B/r \times C \times r \times D} \rightarrow \mathbb{R}^{B \times C \times D}$ and $F_{RS}^{-1}(\mathbf{g}; r) : \mathbb{R}^{B \times C \times D} \rightarrow \mathbb{R}^{B/r \times C \times r \times D}$. Also, the gradient of the tensor repeat operation $F_{RP}(\mathbf{g}; r)$ is the sum of gradients over r : $F_{RP,g}(\mathbf{g}; r) = \sum_{i=1}^r [(\mathbf{g}_i); \dots; (\mathbf{g}_r)] : \mathbb{R}^{C \cdot r} \rightarrow \mathbb{R}^C$. As a result, the gradient for γ and β where the simple case ($D = 1$) become:

$$\frac{\partial \mathcal{L}}{\partial \gamma} = F_{RP,g} \left(\sum_{b=1}^{B/r} F_{RS,g}^{-1} \left(\frac{\partial \mathcal{L}}{\partial \mathbf{y}}; r \right)_b \cdot \hat{\mathbf{h}}_b; r \right), \quad (6)$$

$$\frac{\partial \mathcal{L}}{\partial \beta} = F_{RP,g} \left(\sum_{b=1}^{B/r} F_{RS,g}^{-1} \left(\frac{\partial \mathcal{L}}{\partial \mathbf{y}}; r \right)_b; r \right). \quad (7)$$

Note that both $F_{RS,g}^{-1}(\frac{\partial \mathcal{L}}{\partial \mathbf{y}}; r)$ and $\hat{\mathbf{h}}$ have a reshaped gradient and feature map ($F_{RS,g}^{-1}(\frac{\partial \mathcal{L}}{\partial \mathbf{y}}; r), \hat{\mathbf{h}} \in \mathbb{R}^{B/r \times C \times r \times D}$). As shown in Figure 3(b), if \mathbf{x}^{B_p} contains sampled data from many tasks or is reshaped with enough size of r , the gradient ratio between each previous task’s data and others is changed from $B-1 : 1$ to $B_c/r + B_r/r - 1 : 1$. Finally, the final gradients for β and γ are summed over r . In other words, the gradients become less-biased to the current task because of the tensor reshape operation, and it is further amplified by accumulating these gradients for r times, resulting in a less-biased training of γ and β during backpropagation. Additionally, note that the gradient for γ is also affected by $\hat{\mathbf{h}}$ which is normalized by the task-balanced mean and variance, being more similarly normalized with the test phase.

Implementation details of TBBN There are some considerations to implementing our TBBN in exemplar-based CIL. First, B_c , B_p , and information for the task change are required and the value $\frac{B_c}{B_p}$ must be an integer. However, we believe that these are readily available and adjustable information in a general offline CIL case, as already shown in (Wu et al., 2019; Ahn et al., 2021). Second, not all adaptively determined r can reshape a given feature map. For

example, when $\frac{B_c}{r}$ is not an integer, the tensor reshape operation F_{RS} is not applicable. We overcome this limitation with a simple rule for r . After calculating r by Equation (5) at the beginning of each task training, we set a feasible r^* by following the rule:

$$r^* = \begin{cases} r, & \text{if } r \in CD(B_c, B_p) \\ M(B_c, B_p, r), & \text{otherwise} \end{cases} \quad (8)$$

where $M(B_c, B_p, r) = \max\{\hat{r} : \hat{r} \in CD(B_c, B_p) \wedge \hat{r} < r\}$ and $CD(\cdot, \cdot)$ denotes a set of common divisors between two values. Even though r^* is not the exact optimal value for our TBBN, we will experimentally demonstrate that using r^* is also effective for most CIL experiments at the next section. Finally, note that there is no difference between the original BN and our TBBN in the test phase because TBBN also maintains $\mu, \sigma^2, \gamma, \beta \in \mathbb{R}^C$ in the training phase.

5. Experiments

5.1. Experimental setting

Dataset We evaluate our method with CIFAR-100 (Krizhevsky et al., 2009) and ImageNet-100 (Deng et al., 2009) datasets. With these datasets, we consider two scenarios of CIL, long (10 classes \times 10 tasks, $T = 10$) and short (5 classes \times 20 tasks, $T = 20$) task sequences, respectively for each dataset.

Evaluation Metrics During CL (including CIL), a trained model suffers from the trade-off between stability and plasticity. Therefore, defining a metric for evaluating this trade-off is necessary to evaluate CIL methods well (Masana et al., 2020; Delange et al., 2021; Cha et al., 2020). By following previous works, we use three metrics, Accuracy (Acc \uparrow), Forgetting Measure (FM \downarrow) and Learning Accuracy (LA \uparrow). **Acc** is the metric that measures the classification accuracy of the model for all trained tasks’ test data. **FM** is proposed by (Chaudhry et al., 2018) and it measures the average forgetting of each previous task. **LA** is the metric for comparing the plasticity of the model, proposed by (Riemer et al., 2018), and it is measured by averaging the accuracy of each task when it was first trained.

Experimental details We generally followed the experimental setting proposed in (Masana et al., 2020) and all experiments were done by using their official code. In the case of an experiment for CIFAR-100, we use ResNet-32 (He et al., 2016) for all CIL scenarios but ResNet-18 is used for ImageNet-100. We set the size of exemplar memory to $|\mathcal{M}| = 2000$ at all incremental steps in experiments of both CIFAR-100 and ImageNet-100. For all experiments, we set $m = 0.1$ for the momentum update of running mean and variance. We conducted all experiments in a unified setting for each dataset and scenario. All detailed experimental settings are reported in Supplementary Materials (S.M).

Baselines We selected three common baselines of CIL, such as EEIL (Castro et al., 2018), BiC (Wu et al., 2019), LUCIR (Hou et al., 2019), and implemented them by using the code proposed in the benchmark environment proposed by (Delange et al., 2021). Additionally, we reproduced SS-IL (Ahn et al., 2021), which is one of the current state-of-the-art methods in offline CIL, referring from their official code. Also, we implemented Continual Normalization (CN) (Anonymous, 2022) using the code published by the authors.

5.2. Experimental results for a short task sequence

Table 1: Experimental results with finetuning (FT). All experiments are done by three seeds and we report the average result. Since CN with $g = 32$ causes error when training with ResNet-32, we cannot report the result.

Acc(\uparrow) / FM(\downarrow) / LA(\uparrow)	10 classes \times 10 tasks	
	CIFAR-100	ImageNet-100
FT + BN	36.40 / 47.50 / 79.20	38.72 / 48.80 / 87.52
FT + CN ($g = 2$)	37.89 / 47.90 / 81.00	40.12 / 47.10 / 87.22
FT + CN ($g = 4$)	38.12 / 47.30 / 80.70	41.32 / 46.66 / 87.98
FT + CN ($g = 8$)	37.23 / 49.10 / 81.40	39.74 / 46.98 / 86.72
FT + CN ($g = 16$)	36.03 / 49.30 / 80.90	39.40 / 47.14 / 86.54
FT + CN ($g = 32$)	-	40.60 / 45.98 / 86.58
FT + TBBN	39.86 / 45.60 / 81.00	45.73 / 41.27 / 87.00

Experimental results with finetuning As a first experiment, we conducted experiments of finetuning (FT) with BN, CN, and our TBBN. Table 1 shows the experimental results and we check the following: First, CN does not work well in offline CIL for most g . The author of CN suggested using $g = 8$ and $g = 32$ as the best hyperparameter, however, these are not effective. Also, FT + CN with $g = 2$ and $g = 4$ increase classification accuracy but is not significant. Second, applying TBBN decreases the forgetting of previous tasks, increasing classification performance. Note that searching the hyperparameter is not required for TBBN but it achieves the most superior performance compared to CN with all hyperparameters.

For a more detailed analysis, we investigated a type of misclassification by following the experiment proposed in (Belouadah & Popescu, 2019), and the results are reported in Figure 4. Among four types, $P \rightarrow C$ is called biased prediction and it is known as the main cause of catastrophic forgetting in CIL (Wu et al., 2019; Ahn et al., 2021). As already reported in previous works (Belouadah & Popescu, 2019; Wu et al., 2019), FT + BN suffers from it a lot. However, our TBBN significantly alleviates the biased prediction, resulting in reducing the total number of misclassification. Based on the experimental results, we believe that the bias problem of BN, discussed in Section 4.1, is one of the hidden reasons for causing the biased prediction of CIL, and TBBN can be an appropriate replacement to overcome it.

Experimental results with existing CIL methods Table 2 shows experimental results in the short task sequence. We observe that, first, both BiC and SS-IL achieve superior re-

Table 2: Experimental results for the short task sequence with CIL methods. All experiments are done by three seeds and we report the average result. () shows standard deviation of results and Joint denotes the result trained with including all previous task’s datasets at each incremental step.

Acc(\uparrow) / FM(\downarrow) / LA(\uparrow)	10 classes x 10 tasks (T = 10)	
	CIFAR-100	ImageNet-100
Joint	68.06(\pm 0.40) / 4.80(\pm 1.59) / 71.80(\pm 1.57)	74.99(\pm 0.21) / 4.57(\pm 0.01) / 79.11(\pm 0.13)
FT + BN	36.40(\pm 3.20) / 47.50(\pm 3.48) / 79.20(\pm 0.98)	39.72(\pm 0.88) / 47.52(\pm 1.15) / 87.24(\pm 0.27)
+ CN ($g = 8$)	37.23(\pm 2.76) / 49.10(\pm 1.64) / 81.40(\pm 1.33)	39.91(\pm 0.17) / 47.15(\pm 0.17) / 87.06(\pm 0.34)
+ CN ($g = 16$)	36.03(\pm 1.73) / 49.30(\pm 2.89) / 80.90(\pm 0.72)	40.38(\pm 0.98) / 46.44(\pm 0.70) / 86.82(\pm 0.28)
+ TBBN	39.86(\pm3.06) / 45.60(\pm3.41) / 81.00(\pm1.72)	45.73(\pm0.50) / 40.95(\pm0.70) / 86.68(\pm0.45)
EEIL + BN	39.78(\pm 0.81) / 45.20(\pm 0.98) / 80.50(\pm 1.27)	40.91(\pm 0.95) / 45.87(\pm 1.16) / 86.79(\pm 0.30)
+ CN ($g = 8$)	39.83(\pm 1.23) / 45.90(\pm 2.11) / 81.20(\pm 0.98)	41.13(\pm 0.81) / 45.10(\pm 1.20) / 86.23(\pm 0.39)
+ CN ($g = 16$)	38.46(\pm 0.64) / 46.80(\pm 0.64) / 80.60(\pm 0.76)	42.45(\pm 0.37) / 44.39(\pm 0.31) / 86.84(\pm 0.06)
+ TBBN	44.01(\pm0.23) / 41.50(\pm1.19) / 81.40(\pm0.83)	45.51(\pm0.71) / 41.13(\pm0.66) / 86.63(\pm0.08)
BiC + BN	44.64(\pm 1.53) / 09.70(\pm 1.05) / 52.00(\pm 2.32)	52.50(\pm 0.77) / 11.21(\pm 2.88) / 62.67(\pm 3.00)
+ CN ($g = 8$)	45.24(\pm 1.34) / 09.50(\pm 2.18) / 51.60(\pm 3.72)	53.09(\pm 0.13) / 10.56(\pm 0.50) / 61.94(\pm 0.28)
+ CN ($g = 16$)	44.74(\pm 1.74) / 09.60(\pm 1.36) / 51.20(\pm 2.25)	53.22(\pm 0.34) / 09.73(\pm 0.55) / 61.62(\pm 0.30)
+ TBBN	45.31(\pm1.91) / 09.30(\pm2.25) / 51.60(\pm4.06)	52.01(\pm0.56) / 12.60(\pm3.89) / 64.55(\pm4.54)
LUCIR + BN	38.29(\pm 3.09) / 36.60(\pm 1.86) / 71.30(\pm 1.48)	43.19(\pm 0.10) / 40.87(\pm 0.28) / 84.06(\pm 0.34)
+ CN ($g = 8$)	39.25(\pm 2.31) / 37.00(\pm 1.45) / 72.60(\pm 1.14)	40.96(\pm 0.12) / 41.43(\pm 0.23) / 82.39(\pm 0.11)
+ CN ($g = 16$)	37.10(\pm 3.00) / 38.60(\pm 2.21) / 71.80(\pm 1.01)	41.26(\pm 0.22) / 41.29(\pm 0.23) / 82.55(\pm 0.01)
+ TBBN	41.54(\pm2.40) / 33.90(\pm1.96) / 72.10(\pm1.47)	45.03(\pm0.19) / 38.80(\pm0.08) / 83.83(\pm0.27)
SSL + BN	42.73(\pm 1.18) / 17.40(\pm 0.60) / 57.90(\pm 0.58)	49.29(\pm 0.47) / 19.05(\pm 0.55) / 66.29(\pm 0.42)
+ CN ($g = 8$)	42.62(\pm 1.32) / 15.00(\pm 1.02) / 55.50(\pm 1.42)	50.13(\pm 0.85) / 17.39(\pm 1.21) / 63.42(\pm 0.28)
+ CN ($g = 16$)	41.87(\pm 0.44) / 15.80(\pm 1.27) / 55.40(\pm 2.22)	49.80(\pm 0.46) / 17.94(\pm 0.54) / 63.17(\pm 0.07)
+ TBBN	44.79(\pm0.97) / 19.40(\pm0.44) / 62.10(\pm0.89)	51.49(\pm0.52) / 17.91(\pm0.53) / 68.33(\pm0.24)

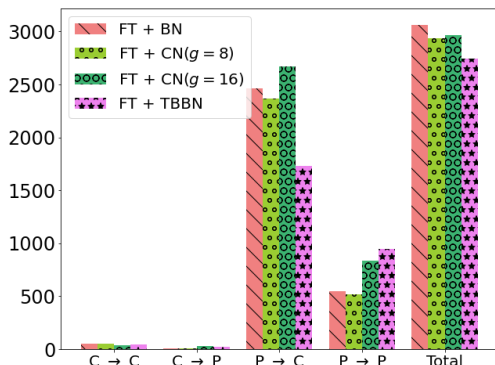


Figure 4: Analysis for four types of misclassification after training the model until the final task ($t = 10$). For example, $C \rightarrow C$ denotes misclassifying a current task’s data ($t = 10$) to another class in the current task, and $C \rightarrow P$ denotes misclassifying a current task’s data to another class in previous tasks ($t = 1, \dots, 9$).

sults than other baselines. Second, as we already checked in the previous section, CN does not work well in most cases. Even though FT + CN shows enhanced performance than FT + BN in some cases (*e.g.*, EEIL + CN in ImageNet-100), it does not improve the performance much and needs to tune different g for each dataset and method, respectively. In contrast, third, TBBN increases classification accuracy (Acc) by reducing the forgetting (FM) in most baselines, except for BiC. We believe it is a remarkable result that the performance of SS-IL, which is one of the state-of-the-art methods, can be further improved by applying TBBN. However, TBBN is not effective for BiC, and this is be-

cause BiC is specialized in correcting the model that makes heavily biased predictions. Finally, FT + TBBN surpasses the performance of EEIL + BN and LUCIR + BN, in both CIFAR-100 and ImageNet-100 datasets. Note that, in the training algorithm of FT + TBBN, there is no distinct solution to overcome catastrophic forgetting or correct biased predictions during CIL. In conclusion, this result demonstrates again that the original BN itself has the problem in CIL, causing biased predictions, as we already discussed in the previous section.

Experiments with other architectures In this section, we verify the effectiveness of TBBN by applying it to more diverse architectures such as ResNet (He et al., 2016), MobileNet (Sandler et al., 2018), ShuffleNet (Zhang et al., 2018), and MnasNet (Tan et al., 2019). We selected four architectures and conducted experiments with ImageNet-100 ($T = 10$), and experimental results are shown in Table 4. The results demonstrate that our TBBN can be generally applied to various architectures and it improves the performance in CIL.

5.3. Experimental results for long task sequence

To further demonstrate an advantage of TBBN in CIL, we consider a more difficult scenario with a greater number of tasks being trained. For CIFAR-100 and ImageNet-100 datasets, we conducted an experiment on a CIL situation in which each task has five classes and the total number of tasks is 20 (5 classes \times 20 tasks).

Figure 3 shows experimental results and the tendency is

Table 3: Experimental results for the long task sequence with CIL methods. All experiments are done by three seeds and we report the average result. () shows standard deviation of results and Joint denotes the result trained with including all previous task’s datasets at each incremental step.

Acc(↑) / FM(↓) / LA(↑)	5 classes x 20 tasks (T = 20)	
	CIFAR-100	ImageNet-100
Joint	69.01(±0.38) / 5.48(±0.50) / 73.39(±1.04)	74.67(±0.05) / 5.99(±0.57) / 79.09(±0.61)
FT + BN	29.66(±1.47) / 52.77(±0.82) / 82.43(±0.65)	38.89(±0.63) / 50.08(±0.48) / 88.97(±0.66)
+ CN ($g = 8$)	35.31(±1.96) / 48.34(±1.11) / 83.65(±0.86)	37.84(±0.39) / 50.75(±0.18) / 88.59(±0.47)
+ CN ($g = 16$)	30.12(±0.30) / 53.22(±0.59) / 83.34(±0.30)	37.40(±0.59) / 50.79(±0.57) / 88.19(±0.38)
+ TBBN	34.56(±2.78) / 49.08(±2.70) / 83.64(±0.08)	43.67(±0.55) / 42.54(±0.57) / 86.21(±0.77)
EEIL + BN	35.11(±0.69) / 46.62(±0.79) / 81.70(±0.12)	37.95(±0.35) / 50.18(±0.44) / 88.11(±0.11)
+ CN ($g = 8$)	35.63(±0.48) / 46.06(±0.42) / 81.61(±0.74)	37.95(±0.49) / 49.64(±0.12) / 87.59(±0.37)
+ CN ($g = 16$)	35.49(±0.89) / 46.08(±0.75) / 81.49(±0.52)	38.33(±0.03) / 49.55(±0.17) / 87.88(±0.20)
+ TBBN	39.32(±0.42) / 42.18(±0.97) / 81.42(±0.72)	42.54(±0.64) / 45.13(±0.71) / 87.61(±0.11)
BiC + BN	36.09(±0.92) / 11.26(±1.35) / 42.60(±1.83)	41.41(±0.41) / 13.55(±2.47) / 50.63(±2.19)
+ CN ($g = 8$)	34.58(±0.11) / 11.16(±2.27) / 38.84(±1.36)	41.63(±0.10) / 14.86(±3.71) / 51.97(±3.87)
+ CN ($g = 16$)	34.77(±0.62) / 11.12(±1.15) / 39.79(±1.71)	41.51(±0.82) / 14.85(±3.28) / 52.01(±4.46)
+ TBBN	34.10(±0.94) / 12.03(±1.48) / 43.42(±2.03)	38.07(±0.43) / 13.43(±2.43) / 49.04(±3.13)
LUCIR + BN	34.36(±0.61) / 40.94(±0.08) / 75.21(±0.78)	39.44(±0.36) / 42.96(±0.66) / 82.31(±0.60)
+ CN ($g = 8$)	33.28(±0.29) / 42.42(±0.89) / 75.47(±0.62)	36.47(±0.87) / 44.97(±0.87) / 81.45(±0.39)
+ CN ($g = 16$)	34.83(±0.07) / 41.20(±0.05) / 75.92(±0.12)	36.54(±0.68) / 44.55(±0.80) / 81.09(±0.13)
+ TBBN	37.07(±0.77) / 39.02(±0.09) / 75.79(±0.78)	39.51(±1.12) / 42.53(±1.38) / 81.94(±0.20)
SSIL + BN	36.31(±1.31) / 21.54(±0.99) / 57.44(±1.41)	43.66(±0.72) / 18.70(±1.01) / 48.49(±0.45)
+ CN ($g = 8$)	35.52(±1.25) / 22.08(±0.70) / 57.33(±0.82)	42.87(±0.34) / 18.67(±0.32) / 45.87(±0.86)
+ CN ($g = 16$)	36.00(±1.07) / 20.88(±0.45) / 56.45(±0.59)	42.95(±0.37) / 18.59(±0.48) / 44.81(±1.08)
+ TBBN	38.55(±0.32) / 22.79(±0.26) / 61.34(±0.06)	46.06(±0.61) / 15.43(±0.55) / 50.69(±0.50)

Table 4: Experimental results with ImageNet-100 using four state-of-the-art architectures.

Acc(↑)	10 classes × 10 tasks			
	ResNet-34	ShuffleNet-v2	MobileNet-v2	MnasNet (x0.5)
FT + BN	40.70	34.36	38.00	36.00
FT + TBBN	46.26	35.08	39.28	37.22

almost the same as previous experimental results in the short task sequence. First, we again check CN does not work except for few cases (e.g., FT + CN ($g = 8$)). Second, TBBN enhances the final performance of most baselines except for BiC. Third, the performance of FT + TBBN in ImageNet-100 surpasses other methods including the current state-of-the-art method, SS-IL. Finally, SS-IL beats BiC in the long task sequence scenario, in addition, applying TBBN to SS-IL boosts its performance of it significantly, achieving the new state-of-the-art performance. Overall, we observe that our TBBN tends to work more effectively in the longer task sequence scenario because, whenever the number of tasks increased, the bias problem of BN becomes more severe.

5.4. Ablation study

Table 5: Ablation study of TBBN in CIFAR-100.

	Task-adaptive r	Task-balanced μ and σ^2	Less-biased learning of γ and β	Acc(↑)
FT + TBBN	✓	✓	✓	39.86
FT + Case 1	✗($r = 16$)	✓	✓	35.64
FT + Case2	✓	✗	✓	38.34
FT + Case3	✓	✓	✗	36.65
FT + BN	✗($r = 16$)	✗	✗	34.47

In this section, we demonstrate the necessity of each proposed component consisting of TBBN via ablation study.

All experiments are done with CIFAR-100 (10 classes × 10 tasks) for three different seeds and we report average accuracy. Table 5 shows the experimental results. When task-adaptive r is not applied, we set $r = 16$ which is the maximum r to be selected by task-adaptive r in the same scenario. As a result of experiments, we confirm that performance degradation occurred whenever each module is removed. Especially, we observe *task-adaptive* r is the most critical component, followed by *less-based learning* of γ and β and *task-balance* μ and σ^2 . The reason, that *task-balance* μ and σ^2 has a relatively small influence compared to other components, is thought to be because of the large similarity between tasks in CIFAR-100. We believe *task-balance* μ and σ^2 would be more effective in a CIL scenario where the task similarity is low. We remain the experiment for it as future work.

6. Concluding Remarks

We propose a simple but effective method, called as Task-Balance Batch Normalization, for exemplar-based CIL. Starting from the analysis on the problem of the original BN, biased mean and variance calculation toward the current task, we devise the novel method to calculate the task-balanced mean and variance for normalization. Also, motivated by GhostBN, we propose the method for less-biased training of parameters for affine transformation and show the analysis for it in terms of a gradient. From extensive experiments with CIFAR-100 and ImageNet-100, we demonstrate that our TBBN can be easily applied to various existing CIL methods, improving their performance further. In the case

of the long task sequence scenario, we observe that simple finetuning with TBBN achieves state-of-the-art performance over the performance of other elaborately designed methods.

References

- Ahn, H., Kwak, J., Lim, S., Bang, H., Kim, H., and Moon, T. Ss-il: Separated softmax for incremental learning. In *Proceedings of the IEEE/CVF International Conference on Computer Vision*, pp. 844–853, 2021.
- Anonymous. Continual normalization: Rethinking batch normalization for online continual learning. In *Submitted to The Tenth International Conference on Learning Representations*, 2022. URL <https://openreview.net/forum?id=vwLLQ-HwqhZ>. under review.
- Belouadah, E. and Popescu, A. Il2m: Class incremental learning with dual memory. In *Proceedings of the IEEE/CVF International Conference on Computer Vision*, pp. 583–592, 2019.
- Bjorck, J., Gomes, C., Selman, B., and Weinberger, K. Q. Understanding batch normalization. *arXiv preprint arXiv:1806.02375*, 2018.
- Bronskill, J., Gordon, J., Requeima, J., Nowozin, S., and Turner, R. Tasknorm: Rethinking batch normalization for meta-learning. In *International Conference on Machine Learning*, pp. 1153–1164. PMLR, 2020.
- Castro, F. M., Marín-Jiménez, M. J., Guil, N., Schmid, C., and Alahari, K. End-to-end incremental learning. In *Proceedings of the European conference on computer vision (ECCV)*, pp. 233–248, 2018.
- Cha, S., Hsu, H., Hwang, T., Calmon, F. P., and Moon, T. Cpr: Classifier-projection regularization for continual learning. *arXiv preprint arXiv:2006.07326*, 2020.
- Chaudhry, A., Dokania, P. K., Ajanthan, T., and Torr, P. H. Riemannian walk for incremental learning: Understanding forgetting and intransigence. In *Proceedings of the European Conference on Computer Vision (ECCV)*, pp. 532–547, 2018.
- Delange, M., Aljundi, R., Masana, M., Parisot, S., Jia, X., Leonardis, A., Slabaugh, G., and Tuytelaars, T. A continual learning survey: Defying forgetting in classification tasks. *IEEE Transactions on Pattern Analysis and Machine Intelligence*, 2021.
- Deng, J., Dong, W., Socher, R., Li, L.-J., Li, K., and Fei-Fei, L. Imagenet: A large-scale hierarchical image database. In *2009 IEEE conference on computer vision and pattern recognition*, pp. 248–255. Ieee, 2009.
- Douillard, A., Cord, M., Ollion, C., Robert, T., and Valle, E. Podnet: Pooled outputs distillation for small-tasks incremental learning. In *Computer Vision–ECCV 2020: 16th European Conference, Glasgow, UK, August 23–28, 2020, Proceedings, Part XX 16*, pp. 86–102. Springer, 2020.
- He, K., Zhang, X., Ren, S., and Sun, J. Deep residual learning for image recognition. In *Proceedings of the IEEE conference on computer vision and pattern recognition*, pp. 770–778, 2016.
- Hoffer, E., Hubara, I., and Soudry, D. Train longer, generalize better: closing the generalization gap in large batch training of neural networks. *arXiv preprint arXiv:1705.08741*, 2017.
- Hou, S., Pan, X., Loy, C. C., Wang, Z., and Lin, D. Learning a unified classifier incrementally via rebalancing. In *Proceedings of the IEEE/CVF Conference on Computer Vision and Pattern Recognition*, pp. 831–839, 2019.
- Ioffe, S. and Szegedy, C. Batch normalization: Accelerating deep network training by reducing internal covariate shift. In *International conference on machine learning*, pp. 448–456. PMLR, 2015.
- Krizhevsky, A., Hinton, G., et al. Learning multiple layers of features from tiny images. 2009.
- Lee, J., Hong, H. G., Joo, D., and Kim, J. Continual learning with extended kronecker-factored approximate curvature. In *Proceedings of the IEEE/CVF Conference on Computer Vision and Pattern Recognition*, pp. 9001–9010, 2020.
- Li, Z. and Hoiem, D. Learning without forgetting. *IEEE transactions on pattern analysis and machine intelligence*, 40(12):2935–2947, 2017.
- Mai, Z. *Online Continual Learning in Image Classification*. PhD thesis, University of Toronto (Canada), 2021.
- Masana, M., Liu, X., Twardowski, B., Menta, M., Bagdanov, A. D., and van de Weijer, J. Class-incremental learning: survey and performance evaluation on image classification. *arXiv preprint arXiv:2010.15277*, 2020.
- Mermillod, M., Bugaiska, A., and Bonin, P. The stability-plasticity dilemma: Investigating the continuum from catastrophic forgetting to age-limited learning effects. *Frontiers in psychology*, 4:504, 2013.
- Parisi, G. I., Kemker, R., Part, J. L., Kanan, C., and Wermter, S. Continual lifelong learning with neural networks: A review. *Neural Networks*, 113:54–71, 2019.

- Rebuffi, S.-A., Kolesnikov, A., Sperl, G., and Lampert, C. H. icarl: Incremental classifier and representation learning. In *Proceedings of the IEEE conference on Computer Vision and Pattern Recognition*, pp. 2001–2010, 2017.
- Riemer, M., Cases, I., Ajemian, R., Liu, M., Rish, I., Tu, Y., and Tesauro, G. Learning to learn without forgetting by maximizing transfer and minimizing interference. *arXiv preprint arXiv:1810.11910*, 2018.
- Sandler, M., Howard, A., Zhu, M., Zhmoginov, A., and Chen, L.-C. Mobilenetv2: Inverted residuals and linear bottlenecks. In *Proceedings of the IEEE conference on computer vision and pattern recognition*, pp. 4510–4520, 2018.
- Santurkar, S., Tsipras, D., Ilyas, A., and Madry, A. How does batch normalization help optimization? In *Proceedings of the 32nd international conference on neural information processing systems*, pp. 2488–2498, 2018.
- Szegedy, C., Vanhoucke, V., Ioffe, S., Shlens, J., and Wojna, Z. Rethinking the inception architecture for computer vision. In *Proceedings of the IEEE conference on computer vision and pattern recognition*, pp. 2818–2826, 2016.
- Tan, M. and Le, Q. Efficientnet: Rethinking model scaling for convolutional neural networks. In *International Conference on Machine Learning*, pp. 6105–6114. PMLR, 2019.
- Tan, M., Chen, B., Pang, R., Vasudevan, V., Sandler, M., Howard, A., and Le, Q. V. Mnasnet: Platform-aware neural architecture search for mobile. In *Proceedings of the IEEE/CVF Conference on Computer Vision and Pattern Recognition*, pp. 2820–2828, 2019.
- Ulyanov, D., Vedaldi, A., and Lempitsky, V. Instance normalization: The missing ingredient for fast stylization. *arXiv preprint arXiv:1607.08022*, 2016.
- Van de Ven, G. M. and Tolias, A. S. Three scenarios for continual learning. *arXiv preprint arXiv:1904.07734*, 2019.
- Welling, M. Herding dynamical weights to learn. In *Proceedings of the 26th Annual International Conference on Machine Learning*, pp. 1121–1128, 2009.
- Wu, Y. and He, K. Group normalization. In *Proceedings of the European conference on computer vision (ECCV)*, pp. 3–19, 2018.
- Wu, Y., Chen, Y., Wang, L., Ye, Y., Liu, Z., Guo, Y., and Fu, Y. Large scale incremental learning. In *Proceedings of the IEEE/CVF Conference on Computer Vision and Pattern Recognition*, pp. 374–382, 2019.
- Zhang, X., Zhou, X., Lin, M., and Sun, J. Shufflenet: An extremely efficient convolutional neural network for mobile devices. In *Proceedings of the IEEE conference on computer vision and pattern recognition*, pp. 6848–6856, 2018.

Supplementary Materials for Task-Balanced Batch Normalization for Exemplar-based Class-Incremental Learning

Sungmin Cha^{1,2} Soonwon Hong¹ Moontae Lee^{2,3} Taesup Moon¹

1. Details for experimental settings

As a common setting, we train the network using SGD with an initial learning rate of 10^{-1} and momentum is set to 0. Also, the mini-batch size is set to 64. The number of epochs and schedule for adjusting the learning rate are differently set for each dataset and scenario. In the case of sampling algorithm, we used random sampling for ImageNet-100 experiments and herding (Welling, 2009; Rebuffi et al., 2017) for CIFAR-100 experiments. All details on experimental settings and information for hardwares are shown in Table 1.

Table 1: Details about experimental settings.

	10 classes \times 10 tasks		5 classes \times 20 tasks	
	CIFAR-100	ImageNet-100	CIFAR-100	ImageNet-100
epochs per task	160	100	160	50
epoch for lr scheduling	[80, 120]	[30, 50, 70, 90]	[80, 120]	[20, 40]
lr decay	1/10	1/10	1/10	1/10
mini-batch size	64	64	64	64
model	ResNet-32	ResNet-18	ResNet-32	ResNet-18
python version	3.7	3.7	3.7	3.7
pytorch version	1.7.1+cu110	1.7.1+cu110	1.7.1+cu110	1.7.1+cu110
CUDA version	11.2	11.2	11.2	11.2
CuDNN version	8.1.1	8.1.1	8.1.1	8.1.1
GPU	TITAN XP	RTX A5000	1080Ti	1080Ti

2. Additional experimental results

Table 2 show the result of comparison for training time. Because of two components consisting of TBBN, TBBN tasks more time than the original BN about the maximum of 22% more. However, note that there is no difference in inference time at the test phase.

Table 2: Comparison for training time.

	CIFAR-100	ImageNet-100
FT + BN	2.3h	12.7h
FT + TBBN	2.6h	15.5h

¹Department of Electrical and Computer Engineering, Seoul National University, Seoul, Republic of Korea ²Fundamental Research Lab, LG AI Research, Seoul, Republic of Korea ³Information and Decision Sciences, University of Illinois at Chicago, Chicago, Illinois, USA. Correspondence to: Taesup Moon <tsmoon@snu.ac.kr>.

References

- Rebuffi, S.-A., Kolesnikov, A., Sperl, G., and Lampert, C. H. icarl: Incremental classifier and representation learning. In *Proceedings of the IEEE conference on Computer Vision and Pattern Recognition*, pp. 2001–2010, 2017.
- Welling, M. Herding dynamical weights to learn. In *Proceedings of the 26th Annual International Conference on Machine Learning*, pp. 1121–1128, 2009.